

Theory and Application of Time-Temperature Parameters

Rate Process Theory and the Development of Parametric Relationships

Much of the early application and evolution of the high-temperature parametric relationships to data for aluminum alloys were carried out during the 1950s and 1960s under the auspices of the MPC, then known as the Metals Properties Council (now the Materials Properties Council). However, the real origins of the relationships go back considerably further.

The “rate process theory” was first proposed by Eyring in 1936 (Ref 1) and was first applied to metals by Kauzmann (Ref 2) and Dushman et al. (Ref 3). It may be expressed mathematically as:

$$r = Ae^{-Q(S)/RT}$$

where r is the rate for the process in question, A is a constant, $Q(S)$ is the activation energy for the process in question, R is the gas constant, and T is absolute temperature.

Over the years from 1945 to 1950, several investigators, including Fisher and McGregor (Ref 4, 5), Holloman (Ref 6–8), Zener (Ref 7), and Jaffe (Ref 8) were credited with recognizing that for metals high-temperature processes such as creep rupture performance, tempering, and diffusion appear to obey rate process theories expressible by the above equation.

In 1963, Manson and Haferd (Ref 9) were credited with showing that all three of the parametric relationships introduced in the section “Introduction and Background” derive from:

$$P = \frac{(\log t) \sigma^Q - \log t_A}{(T - T_A)^R}$$

where P is a parameter combining the effects of time, temperature, and stress; σ is stress, ksi; T is absolute temperature; and T_A , $\log t_A$, Q , and R are constants dependent on the material.

Larson-Miller Parameter (LMP)

For the LMP, Larson and Miller (Ref 10) elected to use the following values of the four constants in the rate process equation:

$$Q = 0$$

$$R = -1.0$$

$$T_A = -460 \text{ }^\circ\text{F or } 0 \text{ }^\circ\text{R}$$

$$t_A = \text{the constant } C \text{ in the LMP}$$

Thus, the general equation reduces to:

$$P = (\log t + C) (T) \text{ or } \text{LMP} = T(C + \log t)$$

This analysis has the advantage that $\log t_A$ or C is the only constant that must be defined by analysis of the data in question, and it is in effect equal to the following at isostress values:

$$C = (\text{LMP}/T) - \log t$$

In such a relationship, isostress data (i.e., data for the same stress but derived from different time-temperature exposure) plotted as the reciprocal of T versus $\log t$ should define straight lines, and the lines for the various stress values should intersect at a point where $1/T = 0$ and $\log t =$ the value of the unknown constant C .

Larson and Miller took one step further in their original proposal, suggesting that the value of constant C (referred to as C_{LMP} hereinafter) could be taken as 20 for many metallic materials. Other authors have suggested that the value of the constant varies from alloy to alloy and also with such factors as cold work, thermomechanical processing, and phase transitions or other structural modifications.

From a practical standpoint, most applications of the LMP are made by first calculating the value of C_{LMP} that provides the best fit in the parametric plotting of the raw data, and values for aluminum alloys, for example, have been shown to range from about 13 to 27.

Manson-Haferd Parameter (MHP)

For the MHP, Manson and Haferd (Ref 9, 11) chose the following values for the constants in the rate process equation:

$$Q = 0$$

$$R = 1.0$$

4 / Parametric Analyses of High-Temperature Data for Aluminum Alloys

Under these assumptions, the general equation reduces to:

$$P = \frac{\log t - \log t_A}{T - T_A}$$

In this case, there are two constants to be evaluated, $\log t_A$ and T_A . Manson and Haferd proposed that isostress data be plotted as T versus $\log t$ and the coordinates of the point of convergence be taken as the values for $\log t_A$ and T_A .

It may be noted that the key difference between the LMP and MHP approaches is the selection of $T_A =$ absolute zero as the temperature where the isostress lines will converge in the LMP while in the MHP T_A is determined empirically, or in effect allowed to “float.”

Dorn-Sherby Parameter (DSP)

Dorn and Sherby (Ref 12) based their relationship more directly on the Eyring rate-process equation:

$$\text{DSP} = te^{-A/T}$$

where t is time, A is a constant based on activation energy, and T is absolute temperature.

This relationship, like the others, implies that isostress tests results at various temperatures should define straight lines when $\log t$ is plotted against the reciprocal of temperature. However, it differs from the other approaches in that these straight-line plots are indicated to be parallel rather than converging at values of $\log t$ and $1/T$.

Observations on the LMP, MHP, and DSP

The essential significance of the differences in the three parameters described previously and applied herein may be illustrated by the schematic representations in Fig. 1 based on the

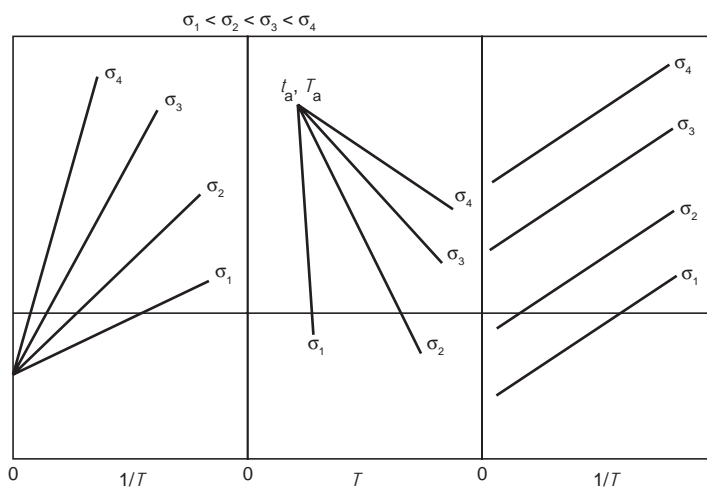


Fig. 1 Comparison of assumed constant stress versus temperature relationships for Larson-Miller (left), Manson-Haferd (center), and Dorn-Sherby (right). T , exposure temperature, absolute; t , exposure time, h ; σ , test/exposure stress.

relationship assumed of the relationships between $\log t$ and $1/T$ (Ref 6).

As noted in the previous discussions, the LMP assumes that the isostress lines converge on the ordinate of a log time versus inverse temperature plot, while the MHP assumes convergence at some specific value of both $\log t$ and $1/T$. The DSP assumes the isostress lines are parallel rather than radiating from a specific value of coordinates $\log t$ and $1/T$.

As representative data illustrated in this book show, the impact of the differences on the results of analyses with the three different parameters is not very great.

It is appropriate to note that a number of variations on the three parameters described previously have been proposed, primarily including such things as letting the values of the various constants, such as the C in the LMP and the activation energy A in the DSP, “float.” None of these have seemed a useful extension of the originals. It is common practice to use the available raw data to calculate or determine graphically the values of the needed constants, but then once established to hold them constant. Allowing the constants in any of the relationships to float, for example, the activation energy in the DSP, results in a different type of analysis in which the isostress lines are curves, not straight lines, and considerably complicates its routine use.

Illustrative Applications of LMP, MHP, and DSP

Several interesting facets of the value and limitations of the parametric relationships may be seen from looking at representative illustrations for the following four alloys and tempers where all three parameters are applied to the same sets of data.

- 1100-O, commercially pure aluminum, annealed (O)
- 2024-T851, a solution heat treated aluminum-copper (Al-Cu) alloy, the series most widely used for high-temperature aerospace applications. The T851 temper is aged to peak strength, so subsequent exposure at elevated temperatures results in overaging, and some microstructural changes may be expected.
- 3003-O, a lightly alloyed non heat treatable aluminum-manganese (Al-Mn) alloy, widely used for heat exchanger applications. It is annealed so no further transitions in structures are anticipated as it is further exposed to high temperatures.
- 5454-O, the highest strength aluminum-magnesium (Al-Mg) alloy recommended for applications involving high temperatures. Because of the higher alloying, there may be diffusion of constituent with high-temperature exposure even in the annealed temper.

Many other alloys and tempers are included in the group for which master parametric relationships are presented in the section “Presentation of Archival Master LMP Curves.”

It is appropriate to note that some components of the following presentations are based on the efforts of Bogardus, Malcolm, and Holt of Alcoa Laboratories, who first published their preliminary assessment of these parametric relationships in 1968 (Ref 13).

Notes about Presentation Format

Generally, plots of stress rupture strength or any other property are presented with the property on the ordinate scale and the parameter on the abscissa, as in Fig. 1100-8. From the descriptions in Chapter 2, all three of the parameters discussed herein include both time and temperature, so it is useful to note that the parametric plots can also be presented as in Fig. 2043-3, 2024-6, or 2024-7, examples of the three parameters in which at the bottom, abscissa scales showing how the combination of temperature and time are represented.

This type of presentation is often useful for individuals using the parameters for extrapolations, but it is not a necessary part of the presentation. Therefore, the multiple abscissa axes showing time and temperature are not included as a general rule through this volume unless the archival version included them.

It is also appropriate to clarify at this stage that the values shown for the Larson-Miller parameter on the abscissas are in thousands and are presented as $LMP/10^3$; thus for example, in Fig. 1100-8, the numbers from 13 to 21 on the abscissa are actually 13,000 to 21,000. For the Manson-Haferd and Dorn-Sherby parameters, the values are as shown.

Alloys 1100-O and H14

Table 1100-1 presents a summary of the stress rupture strength data for 1100-O and 1100-H14; the discussion immediately following focuses on the O temper data. This summary is for rather extensive tests of single lots of material. Other lots of 1100 were also tested, as is illustrated later, but this material was the basis of the best documented master curves for 1100-O and H14. The data are plotted in the format of stress rupture strength as a function of rupture life in Fig. 1100-1 and Fig. 1100-2 for the O and H14 tempers, respectively.

LMP for 1100-O. Figure 1100-3 shows the archival master LMP curve developed for 1100-O derived with a value of the Larson-Miller parameter constant C_{LMP} of 25.3. The isostress calculations leading to the selection of this value of C_{LMP} no longer exist. Scatter and deviations are small, and the curve appears to represent the data reasonably well.

MHP for 1100-O. The isostress plot of $\log t$ and temperature is shown in Fig. 1100-4. The isostress lines are not straight nor do they seem to converge as projected by Manson and Haferd, but values of the constants may be judged from projections of the straight portions of the fitted lines as: $\log t_A = 21.66$ and $T_A = -500$. The resultant master MHP curve is illustrated in Fig. 1100-5. With the exception of several points obtained in tests at 250 °F, the fit is reasonably good.

DSP for 1100-O. Calculations of the activation energy constant for the DSP resulted in a value of 44,100, and the resultant master curve is illustrated in Fig. 1100-6. With the exception of the data for the lower temperatures, the fit is reasonably good.

Comparisons of the Parameters. All three parametric relationships represent data for 1100-O reasonably well. An additional useful comparison test is the degree of agreement in extrapolated values for predicted rupture life after 10,000 and 100,000 h:

Temperature, °F	Desired service rupture life, h	LMP rupture strength, ksi	MHP rupture strength, ksi	DSP rupture strength, ksi
212	10,000	6.0	5.4	5.9
	100,000	5.3	4.0	5.0
300	10,000	3.7	3.0	3.2
	100,000	3.0	2.3	2.7
400	10,000	2.5	2.4	1.9
	100,000	2.1	1.4	1.5
500	10,000	1.1	1.1	1.0
	100,000	<1.0	<1.0	<1.0

There is fairly good agreement among the extrapolated values for the three parameters, usually 1 ksi or less variation. It is notable that the MHP usually provided the lowest extrapolated value, while the LMP provided the highest, usually by less than 0.5 ksi.

Alloy 2024-T851

Figures 2024-1 and 2024-2 provide graphical summaries of the stress rupture strengths of 2024-T851 over the temperature range from room temperature (75 °F, or 535 °R) through 700 °F (1160 °R). The data in Fig. 2024-1 are plotted as rupture strength as a function of rupture time for each test temperature, and those of Fig. 2024-2 are plotted as a function of temperature. The raw test data are tabulated in Table 2024-1, along with the archival isostress calculations.

LMP for 2024-T851. Table 2024-1 summarizes the isostress calculations to determine the LMP constant C_{LMP} for 2024-T851. The calculations show quite a range of potential values for C_{LMP} , ranging from about 13 through 26. It is to be expected that changes in rate-process-type reactions would be in evidence for 2024-T851, as it had originally been aged to maximum strength; subsequent exposure to high temperatures results in increased precipitation of alloying constituents at varying rates and, eventually, recrystallization.

The general tendency is for C_{LMP} to decrease with both longer rupture life and also with increasing temperature. Since the long-life values tend to best represent the range into which extrapolations of data for design purposes are most likely to be needed, there is a general practice to place greater weight on the values of C_{LMP} for longer lives.

Figure 2024-3 is a master LMP curve for 2024-T851 based on an assumed value of $C_{LMP} = 15.9$. To facilitate interpretation, time-temperature pairs are shown along with the LMP values on the abscissa.

Several observations can readily be made. The data for room temperature do not fit with the remainder of the data and are ignored in the analysis. In addition, for each test temperature, the higher shorter-life data plots create “tails” off of the resultant master curve; these fade into the master curve as rupture life increases. The longer-life and higher-temperature data fit rather well into a relatively smooth curve, not surprisingly, given the selection of a value of C deriving most heavily from the longer-life data.

Figure 2024-4 presents the “extrapolated” curves of stress versus rupture life for 2024-T851 utilizing the value of $C_{LMP} = 15.9$.

Additional discussion and illustrations of the effect of varying the values of C are included later.

MHP for 2024-T851. A graphical presentation of the isostress lines of $\log t$ versus T plotted by the least squares method to determine the MHP constant is shown in Fig. 2024-5. There is some variability, especially at the highest and lowest stress values, but a fair convergence of data at values of $\log t = 10.3$, which becomes the value of t_a , and a value of temperature (T_A) of 45 °F (505 °R).

Figure 2024-6 is a MHP master curve for 2024-T851. Aside from the data from room-temperature tests, which have been completely ignored, the fit is quite good. There is no obvious evidence of the “tails” for shorter-life data in the MHP curve.

DSP for 2024-T851. Calculations for the activation energy constant in the DSP, shown in Table 2024-2, yielded a value of 43,300. The resultant master curve derived from analysis with the Dorn-Sherby parameter is illustrated in Fig. 2024-7. Even the room-temperature data may be considered to fit reasonably well, but they were ignored in drawing the main part of the curve. There is some small evidence of shorter-time data resulting in “tails” off the curve, but these are much less pronounced than those for the LMP master curve.

Comparisons for 2024-T851. The master curves for the LMP, MHP, and DSP in Fig. 2024-3, 6, and 7 are useful for making some extrapolations and seeing how they compare. For applications like boilers and pressure vessels it is common to make the best judgments possible for 100,000 h stress rupture strengths, and so in Fig. 2024-8, values of 100,000 h rupture life are shown for a variety of stresses for 2024-T851.

The first overall observation is that of fairly good agreement among the extrapolations based on the three methods. There are subtle differences, however. At higher stresses, the LMP projects 2 to 3 ksi lower (more conservative) rupture stresses than the other two, while at lower stresses, the LMP and DSP provide 2 to 3 ksi higher rupture stresses. Percentagewise, the significance of the differences at lower stresses is fairly substantial. The apparent agreement of the LMP and DSP in this range provides some basis for putting greater faith in those values.

Alloy 3003-O

Figure 3003-1 and 3003-2 provide graphical summaries of the stress rupture strengths for 3003-O over the temperature range from room temperature (75 °F, or 535 °R) through 600 °F (1060 °R). The rupture strengths are plotted in Fig. 3003-1 as a function of rupture time for each test temperature and in Fig. 3003-2 as a function of test temperature.

LMP for 3003-O. The original isostress calculations to determine the C_{LMP} for 3003-O are no longer available. A value of $C_{LMP} = 16$, the archival master LMP curve in Fig. 3003-3 was generated. There is some evidence of the “tails” associated with the short-life test results at lower temperatures, but in total the master curve looks reasonable and represents most of the data well. Another curve was also developed using $C_{LMP} = 17.5$ illustrated in Fig. 3003-4, and the “tails” largely disappear, and a smoother curve is generated.

MHP for 3003-O. Figure 3003-5 illustrates the isostress plot for 3003-O. Convergence is far afield of the plotted data, but values of the constants were judged to be $T_A = -230$ and $\log t_A = 14$.

Figure 3003-6 contains the MHP master curve for 3003-O calculated using the above constants. In this case, “tails” are very much in evidence for the MHP analysis as for the LMP analysis. Nevertheless, a seemingly useful master curve for long-life extrapolations is obtained.

DSP for 3003-O. A DSP activation energy constant of 35,000 was calculated from the 3003-O data, and the derived master DSP curve is presented in Fig. 3003-7. In this instance, the DSP curve, like the LMP and MHP curves, shows clearly the lack of fit of short-life data at several temperatures, but a useful master curve for long-life extrapolation seems to be present.

Comparisons for 3003-O. Once again, the extrapolation to 100,000 rupture life is used as a basis of comparing the results of the three parameters, as illustrated in Fig. 3003-8.

Initial inspection shows fairly good agreement; however, once again there are subtle but perhaps important differences. The LMP and DSP show the best agreement, especially at lower stresses, where the extrapolated values range from about 2 to 4 ksi higher than the MHP extrapolations. There is some evidence that at very low stresses (at or below 2 ksi), the differences are inconsequential.

Alloy 5454-O

Figure 5454-1 provides a graphical summary of the original archival stress rupture strengths for 5454-O as a function of rupture life for each test temperature.

LMP for 5454-O. Table 5454-1 summarizes the isostress calculations to determine the LMP for 5454-O. The range of values of C_{LMP} is relatively narrow, about 11 through 15, and absent any large trends toward higher or lower values at long rupture lives. In this case, a value of C_{LMP} of 14.3, close to the average of all calculations, was used in developing the archival master LMP curve in Fig. 5454-2.

The LMP master curve is relatively uniform and consistent, lacking any significant distortions. Figure 5454-3 presents the raw stress rupture strength versus life data extrapolated based on the LMP master curve in Fig. 5454-2.

MHP for 5454-O. Figure 5454-4 illustrates the isostress plot for 5454-O needed to generate the MHP constants. In this case, there is considerable variation in the shape of the individual isostress lines, and only those for stresses of about 20 or above strongly suggest convergence. Giving more weight to those lines results in values of $T_A = -161$ and $\log t_A = 11.25$.

Figure 5454-5 contains the MHP master curve for 5454-O calculated using the above constants. Despite the difficulties with convergence of the isostress lines, the resulting MHP master curve is relatively uniform and consistent,

DSP for 5454-O. A DSP activation energy constant of 31,400 was calculated, as in Table 5454-2, for the 5454-O data, and the derived master DSP curve is presented in Fig. 5454-6. In this instance, the DSP curve, like the LMP and MHP curves, provides a rather uniform and consistent fit with the data.

Comparisons for 5454-O. Extrapolations for both 10,000 and 100,000 h for 5454-O based on the three parameters are:

Factors Affecting Usefulness of LMP

There are several very basic factors that can influence the variability in the accuracy and precision of properties developed by parametric extrapolation over and above normal test reproducibility. Some are experimental in nature; others are within the analytical and graphical presentations of the data.

Among the most important are the following each of which is discussed in the following section:

- Normal rupture test reproducibility
- Testing laboratory variability
- Lot-to-lot variations for a given alloy/temper/product
- The selection of the constant, C_{LMP} , in the Larson-Miller parametric equation
- The scales and precision of plotting the master curve
- Microstructural changes that occur in the material as a result of the time-temperature conditions to which it is exposed

The opportunity to examine all of these variables exists within the data presented herein.

Normal Rupture Test Reproducibility

One of the most basic factors influencing extrapolations, no matter how they are carried out, is the variability in creep rupture test results run under presumably identical conditions, usually referred to as scatter in test results. In creep rupture tests, the controlled variable is usually the applied stress, and the dependent variable is rupture life at the applied stress.

Data for 5454-O, taken from the extended summary for a single lot of plate of that alloy in Table 5454-4, provide some interesting representative examples of the magnitude of this variation:

Test temperature, °F	Applied creep stress, ksi	Number of replicate tests	Rupture lives, h	Average rupture life, h	Percent range in life from average
350	14	3	64, 75, 106	82	±26
350	11	5	484, 510, 360, 391, 435	436	±17
400	9	7	158, 188, 170, 198, 132, 150, 164	166	±20

An additional opportunity for comparisons of replicate test variability exists in the data for 6061-T651 in Table 6061-1. Some examples from those data are:

Test temperature, °F	Applied creep stress, ksi	Number of replicate tests	Rupture lives, h	Average rupture life, h	Percent Range in life from average
350	21	2	1663, 1912	1788	±14
400	21	6	70, 74, 72, 67, 72, 69	71	±6
450	13	2	177, 257	217	±24
450	13	2	121, 182	152	±20
450	11	2	681, 941	811	±16
500	13	3	11, 23, 33	22	±50
550	8	2	76, 102	89	±15
600	6	2	38,45	234	±8
650	3	2	79, 115	97	±19
700	3	2	15, 20	18	±14
700	2.5	2	181, 227	204	±11

Temperature, °F	Desired service rupture life, h	LMP rupture strength, ksi	MHP rupture strength, ksi	DSP rupture strength, ksi
212	10,000	17	16	17
	100,000	14	10	13
300	10,000	10	8	9
	100,000	7.5	4.1	5.5
400	10,000	4.1	3.5	3.9
	100,000	3.2	2.1	2.5
500	10,000	2.3	2.0	2.1
	100,000	1.9	(a)	(a)

(a) Data do not support extrapolation to this level.

As for the other alloys discussed previously, there is generally fairly good agreement among values extrapolated from the three parameters. However, once again the MHP master curve consistently yielded slightly lower rupture strengths than the other two, and the LMP-based values were generally the highest by a small margin. The divergence was larger for 100,000 h values than for 10,000 h values, as would be expected, and at 300 °F, the divergence was rather significant (a range of 3.4 ksi, about 50%).

Summary of Parametric Comparisons

As noted previously, all three parameters (LMP, MHP, and DSP) provide generally relatively good overall fit to the raw data, other than occasional “tails” resulting from deviations of relatively short-time tests at the lower temperatures from the broader trends. Since the purpose of the parametric analyses is long-life extrapolation, it is most important that the longer-time test data for various temperatures fit a reasonable and consistent pattern.

Also there was generally fair agreement in extrapolated service strengths for 10,000 and/or 100,000 h though the MHP rather consistently projected slightly lower long-time rupture strengths than the other two parameters.

Of the three parametric relationships described previously, the Larson-Miller Parameter (LMP) was chosen as the principal parametric tool to be used by the experts, including those at Alcoa Laboratories, in developing the bases for extrapolations to project creep and rupture strengths for longer lives than practical based on empirical testing. The primary reasoning was that since all three approaches gave similar results within reasonable experimental error (see the section “Testing Laboratory Variability”), the LMP was significantly simpler to use both for calculations of the constant C_{LMP} and for subsequent iterations with different values of C_{LMP} to see how curve fit with raw data was affected. Much of this work was carried out prior to the era of computer generation of master curves and was based on relatively tedious and repetitious hand calculations.

Such analyses were routinely used to generate design values for aluminum alloys for applications such as the ASME Boiler & Pressure Vessel Code (Ref 14).

Subsequently, the data presentations and discussion throughout the remainder of this volume focus on applications of the LMP, and will provide considerable insight into the sources and results of experimental and procedural variability.

These two examples illustrate the fact that ranges in rupture life as great as about $\pm 20\%$ of the average rupture life are likely to be seen in replicate tests, and in some instances, even in very reliable laboratories, ranges of $\pm 50\%$ may occasionally be observed.

These observations suggest that when extrapolating data by whatever means, ranges in average rupture strength at a given rupture life of ± 1 to 2 ksi should not be unexpected. This provides a useful yardstick for comparisons of other test variables and the precision to be expected of extrapolations.

Testing Laboratory Variability

Data for 6061-T651 plate in Table 6061-1 provide a unique opportunity to examine the result of having several different testing laboratories involved in a single program, or in assessing the effect of trying to compare results obtained from several laboratories. Three different experienced laboratories were involved in the program for which the results are presented in Table 6061-1; they are designated simply A, B, and C for purposes of this publication. All three were deep in creep rupture testing experience, and all three inputted data for consideration for design properties for the Boiler & Pressure Vessel Code of ASME (Ref 14).

Some direct comparisons of tests carried out at the same test temperatures and applied creep rupture stresses are summarized in Table 6061-7, together with calculations of the average rupture lives and deviations of the individual values from the averages. For the 18 direct comparisons available for 6061-T651, the average difference in individual tests from the average was 22%, with the individual differences generally ranging from 1% to 41% with one extreme of an 81% difference.

This average difference of $\pm 22\%$ is in the same range as the variation in replicate tests at a single laboratory from the section "Normal Rupture Test Reproducibility," which makes it difficult to say these differences are related to the laboratories or just more evidence of the scatter in replicate tests. At any rate, the use of multiple reliable laboratories does not seem to further increase the variability in creep rupture test data.

One added note: in the lab-to-lab differences summarized in Table 6061-7, Lab A reported longer lives in 14 of the 17 cases where it was compared with Labs B and/or C, and the average difference for those cases alone was $\pm 25\%$, 3% more than the overall average, and possibly significant. It is impossible to say many years in hindsight whether this was related to any basic differences in test procedures, and therefore which of the labs if any generated more or less reliable data. Possible reasons for differences from lab to lab could include variables such as (a) differences in alignment (better alignment leading to longer rupture lives); (b) differences in temperature measurement precision, accuracy, and control; and (c) uniformity of conditions throughout the life of the test.

Lot-to-Lot Variability

Aluminum Association specifications for aluminum alloy products published in *Aluminum Standards & Data* provide acceptable ranges of both composition and tensile properties for each alloy, temper, and product defined therein. Just as multiple lots of the same alloy, temper, and product have some acceptable variation in chemical composition and tensile properties within the appropriate

prescribed specification limits, those lots may also be expected to have some variability in creep rupture properties. The variability may be even greater when different products of the same alloy and temper are included in the comparison.

This is illustrated by master LMP curves developed individually for three lots of 5454-O, one of rolled and drawn rod and two of plate, and illustrated in Fig. 5454-7, 8, and 9, respectively. A composite curve was also developed, and it is shown in Fig. 5454-10. The curves for the separate lots are largely similar in shape and range for both stress and LMP values, but the LMP constants C_{LMP} calculated for the three, ranging from 13.954 to 17.554 (the precision of the original investigators is retained here), with the composite C_{LMP} being 15.375, resulting in three independent curves for the three lots.

Table 5454-6 provides an illustration of the variations in extrapolated service lives of 10,000 and 100,000 h would be influenced by the use of data from any of the individual lots of 5454-O. Despite the use of the three different sets of data for the three different lots, leading to differing C_{LMP} values, it is very interesting and useful to note that the 100,000 h. rupture strengths vary no more than ± 1 ksi from the composite value and are often much less divergent.

Effect of LMP Constant (C_{LMP}) Selection

A very logical concern to the materials data analyst is the effect of variations in the LMP constant selected for the analysis of a specific set of data on the precision and accuracy of extrapolations made based on LMP. This is particularly important as the selection of the LMP constant may be somewhat subjective, especially when cold worked or heat treated tempers are involved.

While there are times when a single specific value of the constant may be indicated by the variety of isostress pairs available for a specific alloy and temper, more often there is a range of LMP values generated, sometimes varying in some manner with temperature and rupture life. The final selection of constant is often made in consideration of the part of the LMP master curve most clearly involved in the extrapolation(s) to be made. In particular, that is often a value of the constant that best fits the long-life data points.

Thus it is useful to examine the effects of variations in the range of LMP constant utilized on the resultant extrapolations, and there are several data sets available to allow that comparison, including 1100-O, 5454-O and H34, and 6061-T6.

Alloy 1100-O. Figure 1100-7 illustrates the master LMP curves for 1100-O plotted using several different values of C_{LMP} based on the calculations in Table 1100-2. Included in the range of C_{LMP} values are the extreme low value of 13.9 observed for 1100-O to the highest value of 25.3 used in the archival plot (Fig. 1100-3). It is apparent from Fig. 1100-7 that on the scale used in this plot, the highest and lowest values of C_{LMP} each lead to a "family" of curves, while the intermediate value, and especially the value of 17.4, provides a relatively smooth relationship reasonably represented by a single curve.

It is useful to see how these four LMP relationships based on the different C_{LMP} values would agree when used for extrapolation for 20 and 50 year service lives. Extrapolated estimated

creep rupture strengths for 1100-O based on these plots are shown in Table 1100-3. Considering the range in C_{LMP} values, there is remarkable agreement among the extrapolated values, especially for the 20 year values. More divergence is noted among the 50 year values, especially at 200 and 250 °F; at higher temperatures, even the 50 year values are usually within ± 0.2 ksi (which is about 10% at the lower levels).

Alloy 2024-T851. It was noted in the section “Illustrative Examples of LMP, MHP, and DSP” that the isostress calculations for 2024-T851 led to a fairly wide range of values of C_{LMP} . Re-examination of the isostress calculations in Table 2024-1 illustrates that there is a pattern to the variation, such that the values generated using isostresses at 37 ksi or higher averaged 21.8 while at isostress below 37 ksi C_{LMP} averaged 16 ksi. LMP master curves have been generated and are presented in Fig. 2024-9 for the two extremes plus the overall average value of 18.4.

All three curves provide a reasonably good fit for the data, but as would be expected the fit at higher stresses is better with the higher value of C_{LMP} , while the fit at lower stresses is better with the lower value of C_{LMP} .

It is useful to see how this difference in selection of C_{LMP} values would affect the extrapolated values for 10,000 and 100,000 h service stresses:

Temperature		Desired service rupture life, H	$C_{LMP} = 16$ rupture strength, ksi	$C_{LMP} = 18.4$ rupture strength, ksi	$C_{LMP} = 21.8$ rupture strength, ksi	From Fig. 2024-4(a), ksi
°F	°R					
212	672	10,000	49.5	49.5	50.0	49.5
		100,000	44.0	45.5	46.5	45.0
300	760	10,000	34.0	35.0	36.5	35.0
		100,000	26.0	28.0	31.0	26.0
350	810	10,000	23.0	24.5	26.5	23.0
		100,000	14.5	17.5	21	15.0
400	860	10,000	13.0	15.0	17.5	14.0
		100,000	8.0	9.0	12.0	8.0
500	960	10,000	5.0	5.0	5.5	5.0
		100,000	3.5	3.5	4.0	4.0

(a) Stress rupture strengths from archival curves generated with $C_{LMP} = 15.9$

While the extrapolated values depend to a considerable extent on how the master curves are drawn through the plotted points, several consistent trends are evident. While there is often fairly good agreement, it can be seen that the extrapolated values trend higher with the higher C_{LMP} values. The good agreement between the values extrapolated from Fig. 2024-T851 and those from the table generated with $C_{LMP} = 16$ is to be expected since the archival calculations were made with of $C_{LMP} = 15.9$. The other trend, also to be expected, is that agreement is better at the shorter-range extrapolation for 10,000 h than for 100,000 h.

This illustrates the care required to generate C_{LMP} values providing optimum fit to the data and to apply great care in drawing the master curve once the raw data are converted to LMP values and plotted.

Alloy 5454-H34. Stress rupture life data for 5454-H34 have been analyzed with two values on C_{LMP} in Fig. 5454-17 and 5454-18. The original archival value of C_{LMP} equal to 14.3 was used to generate Fig. 5454-17, and a more recent review of all the data generated subsequently (and included in Table 5454-5) were used to generate the $C_{LMP} = 17$ used in Fig. 5454-18.

In this case, the projections for rupture strengths at 10,000 and 100,000 h for 5454-H34 plate are:

Temperature		Desired service rupture life, h	LMP; $C_{LMP} = 14.3$ rupture strength, ksi	LMP; $C_{LMP} = 17$ rupture strength, ksi
°F	°R			
212	672	10,000	21	20
		100,000	15	17
300	760	10,000	10	11
		100,000	7.5	8
400	860	10,000	4.1	(a)
		100,000	3.2	(a)
500	960	10,000	2.3	(a)
		100,000	1.9	(a)

(a) Data do not support extrapolation to this level.

The agreement in extrapolated rupture strengths is very reasonable, being ± 1 ksi in all but one case.

Taken together, these examples illustrate that when using the LMP every attempt should be made to obtain the C_{LMP} value providing optimal fit to the data and drawing the master curves carefully. While failure to do so is not likely to greatly mislead the investigator unless the process is pretty badly flawed, it should be recognized that the higher C_{LMP} values are likely to provide the least conservative projections.

Choice of Cartesian versus Semi-log Plotting

Historically, most plotting of parametric master curves has been carried out, using Cartesian coordinates, i.e., with both the property of interest (e.g., stress rupture strength or creep strength) and LMP values on Cartesian coordinates. That was the style used in developing the archival plots included herein, and that focus has been retained throughout most of the book.

However, in some instances investigators find that plotting the property of interest on a logarithmic scale adds precision in the lower values of the property. The potential value of its use may be seen by a comparison of the Cartesian and semi-logarithmic plots for 5454-O in Fig. 5454-13 and Fig. 5454-21, respectively, in both cases using the value of C_{LMP} of 13.9. In the latter, the strengths at high values of LMP are more precisely defined. However, this may have the effect of providing greater confidence than is justified in the extrapolated values in that range.

It is of interest to see what differences are found in the extrapolation of the stress rupture strengths of 5454-O based on the selection of coordinate systems. Using the comparison referenced previously for Fig. 5454-13 and Fig. 5454-21, with the value of C_{LMP} of 13.9, we find the following values of extrapolated stress rupture strength at 10,000 and 100,000 h:

Temperature		Desired service rupture life, h	Cartesian plot $C_{LMP} = 13.9$, ksi	Semilog plot $C_{LMP} = 13.9$, ksi
°F	°R			
212	672	10,000	18.0	18.0
		100,000	14.0	14.5
		1,000,000	11.0	11.0
300	760	10,000	10.0	10.0
		100,000	7.2	7.4
		1,000,000	5.0	5.2
400	860	10,000	4.5	4.7
		100,000	3.4	3.4
		1,000,000	2.6	2.5
500	960	10,000	2.5	2.5
		100,000	2.0	1.8

In the case of such well-behaved data as generated for 5454-O, the semi-log plot does indeed seem to provide added precision to the extrapolation, but the values themselves differ very little from the two types of analyses.

As we see in the section “Software Programs for Parametric Analyses of Creep Rupture Data,” the semi-logarithmic plotting has been incorporated into some parametric creep analysis software. There is also an opportunity to see the impact when the data generated do not provide as fine a fit as do the data for 5454-O.

Choice of Scales and Precision of Plotting

Comparison of the curves in Fig. 1100-3 and 1100-7 also provides an excellent illustration of how important the choices of plotting scales and precision can be. The raw data that went into these two plots are identical, but the differences are rather profound.

While the fit in Fig. 1100-3 looks quite reasonable, it is clear from looking at Fig. 1100-7 that the good appearance of Fig. 1100-3 is based on the high level of compression of the ordinate. Figure 1100-7 illustrates that with $C_{LMP} = 25.3$, the master curve is actually a series of parallel but offset lines for the individual temperatures. This contrasts with the curve for $C_{LMP} = 17.4$, which can be well represented as a single relationship at these scales.

It is interesting to note also that extrapolation with the curve in Fig. 1100-7 for $C_{LMP} = 25.3$ (see Table 1100-3) provides rather good agreement with the better-fitted curves if the extrapolation is carried out using the individual curves for the temperature of interest and extends it parallel to the higher-temperature curves.

Effect of How the LMP Master Curves are Fitted to the Data

The final step in creating the master curve in any parametric analysis of any type of data is drawing in the master curve itself. This can be done mathematically, based on least squares representation or a polynomial equation providing best mathematical fit, but that may not provide the best curve for relatively long-time extrapolation, as noted in the discussion of selection of the constant in the parametric equation.

Some examples of this are apparent in the master LMP curves for Fig. 2024-3 and 6061-3 for the aluminum alloys 2024-T851 and 6061-T651, respectively. Any calculations based on all of the data points in either case would not have provided the desired effect of bringing the relatively longer-time data into good relationship for extrapolation. Fairing the curve with graphical tools such as French curves is usually the step chosen in the final analysis.

However, fairing in the perceived best-fit curve is not always an easy change, especially when the variation in the data, such as a single value of the parametric constant, C_{LMP} in this discussion, provides a smooth fit throughout. The investigator must recognize those cases where it is possible to “shade” the master curve one way or the other depending on the weight given individual data points when it is not clear which may be outliers. It is good practice to examine the effect of different renderings of the master curve fit on the extrapolated values.

Applications When Microstructural Changes are Involved

As noted earlier, one of the challenges in using the Larson-Miller Parameter (and any other time-temperature parameter as well) is dealing with high-temperature data for an alloy-temper combination that undergoes some type of microstructural transition during high-temperature exposure. Examples would include highly strain-hardened alloys, such as non heat treatable alloy 3003 in the H14 to H18 or H38 tempers (i.e. highly cold worked), or heat treated alloys, such as 2024 or 6061 in the T-type tempers (i.e. heat treated and aged).

Once again, there are some useful examples in the datasets included herein, namely, 2024-T851 and 6061-T651.

Alloy 2024-T851. As discussed in the section “Effect of LMP Constant (C_{LMP}) Selection,” the isostress calculations included in Table 2024-1 show a fairly dramatic and consistent decrease in C_{LMP} values with increasing temperature and time at temperature, effectively increasing LMP value. As illustrated in the right-hand column of Table 2024-1, at stresses at or above 37 ksi, an average value of 21.8 represents the data well, but at lower stresses, a C_{LMP} value of 16 is indicated; the overall average value is 18.4.

This is an illustration of the transition from a precipitation-hardened condition through a severely overaged condition to a near fully annealed and recrystallized condition for 2024, with a significant change in C_{LMP} value associated with the initial and later stages.

As illustrated in Fig. 2024-9, the use of the average or lower C_{LMP} values generally results in the best fit for extrapolations involving higher LMP values. Also, as illustrated in the discussion of 2024-T851 in the section “Effect of LMP Constant (C_{LMP}) Selection,” the lower values of C_{LMP} also result in the more conservative and consistent extrapolated stress rupture strengths.

Alloy 6061-T651. Thanks to a cooperative program between Alcoa and the Metals Properties Council MPC, now known as the Materials Properties Council, Inc.), the extensive set of data available for 6061-T651 is also available to illustrate this point (Ref 5).

Table 6061-1 summarizes the stress rupture strength data from the creep rupture tests of 6061-T651 carried out over the range from 200 through 750 °F, an unusually large range, and in several instances replicate tests were made to identify the degree of data scatter that might be expected. These data are plotted as a function of time at temperature in Fig. 6061-1. The isostress calculations for these data are represented in Table 6061-2. Because of the extensive range of data, an unusually large number of isostress calculations were possible and used.

As illustrated in Table 6061-2, a wide range of C_{LMP} values were indicated, and for 6061-T651 as for 2024-T851, there was a transition in the range of values from an average of about 20 (range 17–22) at higher isostresses to around 14 (range 9–18) for lower isostresses, the transition occurring at isostresses of about 6–9 ksi, or around 600 °F. This is consistent with the fact that in this temperature range and above, 6061 would undergo a microstructural transition from the precipitation-hardened condition to that of an annealed condition (effectively going from T6 to O temper).

Once again, the challenge in such a situation is the selection of what C_{LMP} value to use. It is also reasonable to try an approach to

selection of the C_{LMP} value that reflects the transition, that is, to calculate the master curve using both the higher and lower C_{LMP} values plus an overall average. From these data for 6061-T651, values of 20.3 and 13.9 were selected for the higher and lower ranges, respectively, and a value of 17.4 for the overall average.

The three master plots generated using the three values of C_{LMP} are presented in Fig. 6061-3. Not surprisingly, the quality of the plots in terms of fit to the data varies, with the higher and medium C_{LMP} values illustrating better fit at higher stresses and the lower C_{LMP} value providing better fit at the lower stresses. Actually, the fit with the average C_{LMP} value is reasonably good over the entire range.

The next test of the approach becomes to see the effect on the extrapolated values of rupture strength for 6061-T651 for service lives of 10,000 and 100,000 h at various temperatures. The results of the use of the three different C_{LMP} values in extrapolating the stress rupture strengths of 6061-T651 plate are:

Temperature °F	°R	Desired service rupture life, H	$C_{LMP} = 13.9$ rupture strength, ksi	$C_{LMP} = 17.4$ rupture strength, ksi	$C_{LMP} = 20.3$ rupture strength, ksi
212	672	10,000	35.0	35.0	35.5
		100,000	31.0	32.0	33.5
300	760	10,000	23.0	24.0	25.0
		100,000	16.4	18.0	20.0
350	810	10,000	15.5	16.0	17.5
		100,000	10.0	12.0	14.0
400	860	10,000	10.0	11.0	12.5
		100,000	6.5	8.5	9.5
500	960	10,000	6.5	8.0	8.5
		100,000	4.0	5.0	5.5

Several trends are evident:

- Extrapolated rupture strengths at 10,000 and 100,000 h tend to increase with increase in C_{LMP} value.
- The greatest range observed is for 100,000 h extrapolation at 300 and 350 °F, about 4 ksi; for the 10,000 h extrapolations, the range is usually 2 ksi or less.
- Use of the average value of C_{LMP} provides about a good estimate of the average extrapolated stress rupture strength.

How to Apply LMP with Microstructural Conditions. These illustrations suggest that despite the fact that microstructural changes take place as aluminum alloys are subjected to a wide range of time-temperatures exposures, and these changes lead to a relatively wide range or shift in C_{LMP} values, the parametric approach to analysis of the data is still potentially useful and may be applied with care. The presence of such transitions does not eliminate the need to get all the help one can in extrapolating to very long service lives; it in fact exaggerates the value of using this additional tool among others that may be available.

As noted previously, the greatest challenge in such cases is the decision of which value of C_{LMP} for should be used in the analysis. The examples cited previously provide two most useful options:

- Place the greatest emphasis on those values reflecting the temperature range for which predictions are needed. In other words, use the C_{LMP} value that best fits the region in which the extrapolated values are likely to fall, i.e., the C_{LMP} reflecting longer times at the lower temperatures if extrapolations at 150, 212, or 300 °F are involved, and the C_{LMP} reflecting the higher

temperatures or extremely long times at intermediate temperatures if the extrapolations are at 350 °F or above.

- Use the average value of C_{LMP} for all extrapolations; generally the variations will be less than ± 1 ksi.

Illustrations of Verification and Limitations of LMP

It is crucial to be able to characterize the usefulness of parametric extrapolation via LMP or any other in terms of the expected accuracy for long service applications. Yet there is seldom the opportunity to carry out creep rupture tests over the 10 to 20 years needed to judge quantitatively how accurate are extrapolations based on tests carried out for only 100 to 5000 h.

Among the steps taken by Alcoa in cooperation with the Materials Properties Council and the Aluminum Association in the 1960s was the conduct of creep rupture tests anticipated to result in rupture lives at or beyond 10,000 h (Ref 13, 15). The tests were carried out at Alcoa Laboratories and at the University of Michigan using carefully controlled procedures and protected surroundings such that the testing machines and strain recording equipment were minimally disturbed throughout the multiyear duration.

Several illustrations of the results of these studies are re-examined below, with very interesting and useful results. In each case illustrated, the short-time (<10,000 h rupture life) are analyzed independently using the available isostress calculations to generate a value of C_{LMP} that would have been determined if only those short-life data had been available. Then the long-life data (>10,000 h rupture life are examined to determine the degree to which extrapolation of the short-life data would have accurately predicted the very long-life results.

Alloys 1100-O and H14

Table 1100-4 summarizes the short-life (<10,000 h) rupture strengths for 1100-O and H14, and Tables 1100-5 and 6 present the isostress calculations based on those short-life data for 1100-O and H14, respectively. With the exception of two apparent outliers for the O temper associated with one test a 300 °F, a value of $C_{LMP} = 18.2$ is strongly indicated for both tempers. That value was used to calculate the LMP values in Table 1100-7, and the master curves in Fig. 1100-7 (O temper) and 1100-8 (H14 temper) were generated.

For 1100-O, the long-life data (>10,000 h rupture life) are presented in Table 1100-8. Also included in the second block of columns in Table 1100-8 are the LMP values and the extrapolated stress rupture strengths for the observed long-time test results derived from the curve in Fig. 1100-7 that was based on only the short-life data and $C_{LMP} = 18.2$.

The very long time extrapolated rupture strengths for 1100-O are in extremely good agreement with the actual stress rupture lives. To the precision available at the scales used, the extrapolated values were essentially equal to the original test values. In the worst cases, the predicted stress rupture strengths were within ± 1 ksi (± 7 MPa).

It is useful to note that 1100-O represents a material that was annealed, i.e., fully recrystallized prior to any testing, and so it would not undergo any significant microstructural changes during the span of time-temperature tests, even at very high temperatures.

12 / Parametric Analyses of High-Temperature Data for Aluminum Alloys

Therefore, to explore the degree to which short-life data extrapolations for a strain-hardened temper of 1100 would correctly predict long-life test results, parallel sets of calculations were performed for 1100-H14. The short-life data are presented in Table 1100-5, the isostress calculations in Table 1100-6, and the master LMP curve based on the calculated $C_{LMP} = 18.2$ is presented in Fig. 1100-8. The long-life data for 1100-H14 are summarized in Table 1100-9, along with the extrapolated values. In this case, there was perfect agreement between actual test stresses and extrapolated rupture strengths.

Thus, for moderately strain-hardened aluminum alloys as well as annealed aluminum alloys it appears that the LMP approach to extrapolation is rather reliable.

Alloy 5454-O

The fairly extensive data set for stress rupture strength of 5454-O in Table 5454-3 offers another opportunity to check the ability to project long-life rupture strengths from relatively short-life test results. In Table 5454-6, the data from stress rupture tests lasting less than 5000 h were used to generate the constant C_{LMP} for the LMP; it was 13.5, compared to the value of 14.3 used in the archival analysis or 13.9 in a more recent analysis. In the lower part of Table 5454-6, the results of stress rupture test lasting 10,000 h or more are summarized, along with the values that would have been predicted for stress rupture strength by extrapolation using the LMP analysis generated solely from the short-time tests. The analysis is complicated a bit by the fact that about half of the long-life tests were discontinued before failure was obtained.

As might have been expected, given the small variation in C_{LMP} value (13.5 versus 13.9 or 14.3), there is generally very good agreement between the actual and predicted long-life stress rupture strengths, often less than ± 1 ksi. The principal exception was the stress rupture life at 20 ksi, for which the extrapolations with all three values of C_{LMP} were about 17 ksi. This suggests that the test result for 20 ksi was an outlier, not representative of the majority of the data. That assumption is supported by the fact that the test result for 20 ksi at 212 °F was much longer than the comparable values at 300 and 400 °F based on their LMP values.

Incidentally, it appears from the analysis that most of the tests that were discontinued were relatively close to failure lives, that is, of course, on a logarithmic scale, so several thousand more hours might have been involved.

Alloy 6061-T651

As illustrated in the section “Factors Affecting Usefulness of LMP,” alloy 6061-T651, for which data are shown is one of many aluminum alloys and tempers that would be expected to undergo some microstructural change over the range of time-temperature test conditions. Fortunately, the planners of the creep rupture program referenced here (Ref 13, 15) considered these factors and planned tests to determine the stress rupture strengths for lives greater than 10,000 h. Table 6061-1 includes those long-time test results, along with LMP calculations for the three values of C_{LMP} derived from the data considering the lower and higher test temperatures and the overall average value. Some of the long-time tests were discontinued for some reason, and these are included with the appropriate indicators.

For purposes of this study, values of C_{LMP} were calculated using only the stress rupture lives from tests in which the time to rupture was less than 10,000 h. LMP master curves were generated using only the short-life data (<10,000 h) and are presented in Fig. 6061-3 utilizing the three values of C_{LMP} associated primarily with low-temperature test, high-temperature tests, and the overall average.

Table 6061-6 includes the extrapolated stresses from each of the three LMP master curves obtained using the LMP values C_{LMP} associated with the long-time stress rupture life values. Comparison of the values in the Test Stress column (the third column) with the three Extrapolated Stress columns provides an indication of the degree of consistency between actual test results and extrapolations based on the shorter life data (mostly less than 1000 h). Actually a remarkable degree of agreement is found, seldom more than 1 ksi disagreement, and perhaps the best agreement is with the LMP master curve generated with the overall average values C_{LMP} .

These results in general would indicate that the LMP approach has some value as an indicator of long-time life expectations even in situations where transitions in microstructure may occur over the course of time-temperature conditions in the tests.

Limitations of Parametric Analyses

The principal limitations of parametric analyses of creep rupture data are of four types:

- Insufficient raw data to generate adequate isostress calculations for C_{LMP}
- Problems with compressed scale plotting
- The tendency to extrapolate the extrapolation
- Difficulties in getting a suitable fit for the parametric relationship involved with the raw data

These are each discussed briefly below using the LMP analyses to illustrate the points.

Limitation 1: Insufficient Raw Data to Generate Adequate Isostress Calculations for C_{LMP} . As described in the illustrations of how to carry out parametric analyses in the sections “Rate Process Theory and the Development of Parametric Relationships” and “Illustrative Applications of LMP, MHP, and DSP,” the first requirement is for adequate data to carry out isostress calculations to generate constants for the equations, C_{LMP} in the case of LMP. The most useful isostress calculations result from tests at the same creep rupture stress at two or more different temperatures. However, the same effect can be obtained by having overlapping test stresses at different temperatures so that isostress value may be judged by interpolation of data at two different stresses. The optimum situation is to have multiple opportunities across the whole temperature range over which tests were made, sufficient to see if a single value or narrow range of values will provide a good fit for much of the data.

The inability to make at least such calculations can lead to difficulties in moving forward with the analysis. In that event, the appropriate first step would be to try the nominal value of $C_{LMP} = 20$ as suggested in the original analysis by Larson and Miller. In general, the values of C_{LMP} for creep and stress rupture data for aluminum alloys range from 13 to 17, so the value of 20 will provide a good first step.

After the master LMP curve for $C_{LMP} = 20$ has been generated, it is relatively easy to judge whether a higher or lower value of C_{LMP} would improve the fit. Reference to Fig. 1100-7 provides some guidance in this respect:

- If data for individual temperatures are more right-to-left in position as test temperature increases, as for $C_{LMP} = 13.9$ in Fig. 1100-7, the value of C_{LMP} is too low and a higher value should be tried.
- If data for individual temperatures are more left-to-right in position as test temperature increases, as for $C_{LMP} = 25.3$ in Fig. 1100-7, the value of C_{LMP} is too high and a lower value should be tried.

Limitation 2: Problems with Compressed Scale Plotting. As noted in the section “Factors Affecting Usefulness of LMP,” among the variables influencing the precision and accuracy of LMP analyses is the scale of plotting the test results. Plotting on relatively compressed scales for either creep or stress rupture strengths or for the LMP values themselves will have the effect of minimizing scatter in the plot, possibly obscuring the fact that the fit of the raw data is not very good. This tendency of compressing the scatter may give the incorrect impression that good fit has been achieved and introduce more variability in any extrapolated values than desired.

To maximize the value of the analysis, it is best to use as expanded scales as possible given the range of test results and LMP values, giving the best opportunity to recognize temperature-to-temperature variations.

Limitation 3: The Tendency to Extrapolate the Extrapolation. The principal purpose of the development of a master curve is to permit extrapolations of raw data to time-temperature combinations not represented by the raw data themselves. With a good fit of the data, there is good evidence that is a reasonable thing to do.

What is not recommended is to extrapolate beyond the limits of the master curve itself, at least not significantly. To do so places the investigator in a position where there are no data to support the extrapolation, and one may miss a gradual positive or negative change in slope of the extrapolated curve.

Limitation 4: Difficulties in Getting a Suitable Fit for the Parametric Relationship Involved with the Raw Data. As noted in several points discussed previously, the principal challenge in developing LMP master curves or any other type of master plot, is the generation of suitable constants for the parametric relationship, C_{LMP} for the LMP function. While in some cases, reasonably uniform values will be generated from isostress calculations (see Table 5454-7), in other cases rather divergent values may be found (see Table 6061-2).

Even in such cases, there often is a pattern that can be used to judge the most useful value of C_{LMP} . In the case of 6061-T651, it was found that the overall average handled the data quite well in general, as illustrated in Fig. 6061-3. In other cases, it may not be so clear.

Experience has shown that when it is difficult to establish a good average value of C_{LMP} that fits all of the data well, it is best to bias the value of constant to best fit the longer-time data at several test temperatures. This is especially true when the principal purpose of the master curve is to extrapolate to longer times at the

individual temperatures, so the master curve is best based on data representing the longest times and highest temperatures involved. Figure 6061-3 is also a good illustration of that point.

In cases where the extrapolations of principal interest are those at the lowest temperatures, say 150 to 212 °F (65 to 100 °C), it is probably best to use a value of C_{LMP} generated from that range of temperatures if it differs much from the overall average value.

Presentation of Archival Master LMP Curves

Representative archival LMP master curves for the stress rupture strengths and, where available, the creep strengths at 0.1%, 0.2%, 0.5%, and 1% creep strain for the alloys and tempers are presented in the Data Sets at the end of this book.

Those master curves referred to as “archival” are from Alcoa’s archives and are presented here as derived by Alcoa research personnel: principally, Robert C. Malcolm III and Kenneth O. Bogardus, under the management of Alcoa Laboratories division chiefs Francis M. Howell, Marshall Holt, and J. Gilbert Kaufman. This is the group of Alcoa experts, most notably Malcolm, Bogardus, and Holt, who did much of the original analysis leading to the creep design values for aluminum alloys used in publications such as the ASME Boiler & Pressure Vessel Code (Ref 15). The majority of all of the calculations were performed by Malcolm, a heroic task in the days before desktop computers and Lotus or Excel software.

It is appropriate to note that all creep rupture testing for which data are presented herein were carried out strictly in accordance with ASTM E 139, “Standard Method of Conducting Creep, Creep Rupture, and Stress Rupture Tests of Metallic Materials,” *Annual Book of ASTM Standards*, Part 03.01.

Wrought Alloys

- 1100-O, H14, H18: stress rupture strength and, for the O temper, creep strengths
- 2024-T851: stress rupture strength
- 2219-T6, T851: stress rupture strength
- 3003-O, H12, H14, H18: stress rupture strength
- 3004-O, H34, H38: stress rupture strength
- 5050-O: stress rupture strength
- 5052-O, H32, H34, H38: stress rupture strength
- 5052-H112, as-welded with 5052 filler alloy: stress rupture strength
- 5083-H321, as-welded with 5083 filler alloy: stress rupture strength
- 5154-O: stress rupture strengths
- 5454-O, H34, as-welded H34: stress rupture strength and, for the O temper, strength at minimum creep rate
- 5456-H321, as-welded with 5556 filler alloy: stress rupture strength
- 6061-T6 and T651: stress rupture strength, creep strengths, and strength at minimum creep rate
- 6061-T651, as-welded with 4043 filler alloy: stress rupture strength
- 6061-T651, heat treated and aged after welding with 4043: stress rupture strength

14 / Parametric Analyses of High-Temperature Data for Aluminum Alloys

- 6061-T651, as-welded with 5356 filler alloy: stress rupture strength
- 6063-T5 and T6: strength at minimum creep rate

Casting Alloys

- 224.0-T62: stress rupture strength
- 249.0-T62: stress rupture strength
- 270.0-T6: 0.2% creep strength
- 354.0-T6: stress rupture strength
- C355.0-T6: stress rupture strength

Where possible, the more significant sets of raw data used in the parametric analyses, especially for stress rupture strength, are also presented herein. It is important to recognize that data other than the tabular data presented here were also likely to have been considered in the final decisions about design values for any purposes (Ref 14), and the data presented herein should be considered representative of the alloys and tempers but not the sole source of information for any statistical or design application.

As noted earlier, in presenting the LMP master curves, the term “archival” is used in the titles when the curves being presented are reproductions of the results of the original analyses by the Alcoa Laboratories experts noted previously. In these presentations, the precision of the values shown for the LMP constant C_{LMP} are those used by the original experimenters and analysts; in some cases these are round numbers (e.g., 19 or 20), while in others as much as three decimal places (e.g., 17.751) are used. Generally, the calculations on which the original values of C_{LMP} were based are no longer available, and it should be recognized that new investigators using the same data might elect to utilize different values of C_{LMP} .

Also included with the archival curves for the alloys and tempers listed previously are some current LMP parametric plots made by the author using the archival raw data to illustrate some points about the usefulness and limitations of parametric analyses. Those curves are not referred to as “archival.” Those too should be considered as representative of the respective alloys, not of any statistical or design caliber.

As noted previously, the English/engineering system of units is given greater prominence in the tabular and graphical presentations herein because all of these data and the archival plots were generated in that system. For those interested in more information of the use of SI/metric units in parametric analysis, reference is made to Appendix 4.

Software Programs for Parametric Analyses of Creep Rupture Data

While the availability of spreadsheet software programs such as Excel make the calculations involved in the application of parametric analyses such as the LMP to creep rupture data much more efficient and effective than before such programs were available, there have been some significantly greater strides made in this area more recently. A specific example chosen to illustrate this capability is the Granta MI program module known as the “Creep Data Summary” within the MI:Lab database program (Ref 16).

Granta’s MI:Lab is a sophisticated material property data storage, analysis, and reporting program developed by Granta Design, Ltd. of Cambridge, England. Its application modules include tension, compression, relaxation, fracture toughness, and fatigue crack propagation in addition to creep and stress rupture data, the focus of this discussion. It encompasses statistics and graphics among its analytical tools and incorporates database components suitable for all structural materials including composites.

Focusing on the creep and stress rupture capability of Granta MI:Lab, Fig. 2 illustrates which components of the system would be employed, looking at the opening screen of the program. The creep test data are put into the database, and the data are analyzed with the statistical programs with output to the creep summary builder. Users have the ability to use either the Larson-Miller Parameter (LMP) or hyperbolic tangent fitting as models for analysis. For purposes of this volume, focus is given in the following information to the LMP option.

In order to illustrate the application of this program to actual data for an aluminum alloy, data for 2219-T6 forgings, heat treated and aged at 420 °F, from Ref 17 were put through a representative analysis in the MI:Lab creep module. While the data in Ref 17 are not raw test data, but rather typical values gleaned by analysis of many individual test results as described previously in this volume, the usefulness of the evaluation is clear.

To start the process, the stress rupture data for 2219-T6 forgings from Ref 17 were imported via Excel spreadsheet to the MI:Lab module from the ASM Alloy Center on the ASM International website (Ref 18). These same values are shown in Table 2219-1. The individual doing the analysis has several decisions to make to begin the process, including (a) which model to use, LMP or hyperbolic tangent (tanh), (b) which creep rupture variable to use, in this case, stress at time to rupture, or stress rupture strength; (c) which C_{LMP} value (called K in this software) to use, and (d) the number of terms desired in the polynomial equation for the fit.

Once these variables are set, the program proceeds with the analysis and provides the user with the summary presentation of the information illustrated in Fig. 3. That summary includes:

- On the right is a summary of the numeric results of the analysis for the C_{LMP} .
- Upper left shows plots of the stress rupture strength data for each temperature as a function of time to rupture.
- Lower left shows plots of the LMP (called K in the program) for each temperature as a function of rupture life.
- In the center is the resultant master LMP curve, both average best fit parabolic equation with the requested number of terms, and minimum, based on the safety factor the user prescribes. Note that the Granta MI:Lab software presents the LMP master curve in semi-log coordinates, as discussed in the section “Choice of Cartesian versus Semi-log Plotting,” and the units used in the software are SI/metric.

This final semi-log LMP master curve from the Granta MI:Lab software is also presented on a larger scale as Fig. 2219-2. Here the first of two limitations to this software are noted, as the scales and lack of intermediate scale division lines make interpolation within the plot to any great precision rather difficult. The software

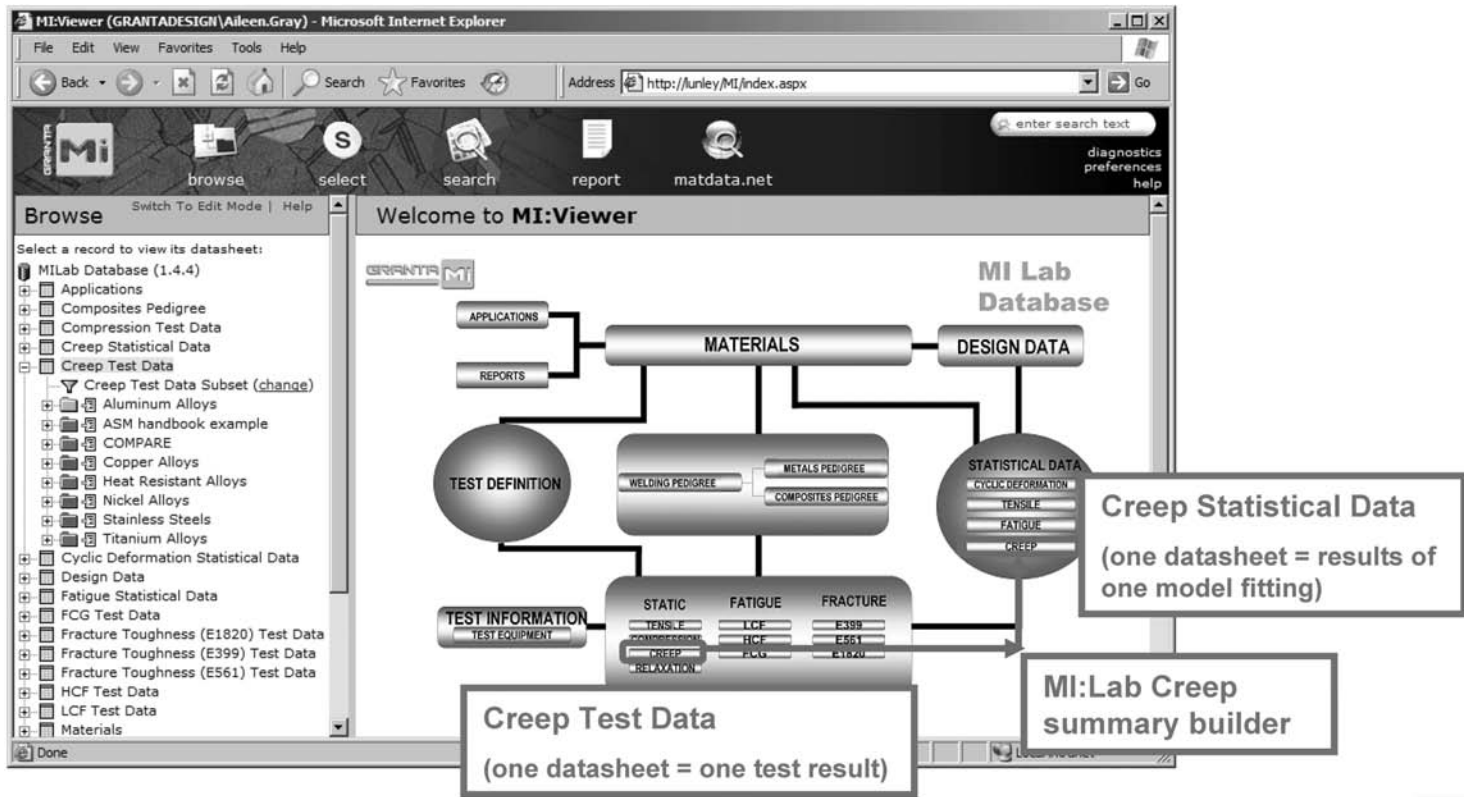


Fig. 2 Initial computer screen of Granta MI:Lab Database Software System, introducing components of the Creep Summary Module

output would be better served to include a larger-scale plot with finer scale division.

For comparison, the short-time (up to 1000 h rupture life) stress rupture data from which this plot was generated are summarized in Table 2219-2, and isostress calculations were made to determine if a better fit might be obtained with a value of C_{LMP} other than the 20 used arbitrarily in the MI:Lab analysis. It is interesting to note that isostress analysis of the archival data for 2219-T6 forgings in Table 2219-2 led to an average C_{LMP} value of 24.7 rather than the nominal value of 20 selected for the MI:Lab analysis. This illustrates the second shortcoming of the MI:Lab creep software, as it would be a valuable enhancement to users for the software to make the isostress calculations as part of the analysis and draw the master curve with an optimized value rather than rely on the investigator's judgment or separate analysis.

As an added comparison, Fig. 2219-3 includes semi-log master curve plots for values of C_{LMP} of both 20 and 24.7. While the overall fit is clearly better with the higher value of C_{LMP} , it is also clear that neither takes very well into account the shorter-time tests at 700 °F. This is a good illustration of the point made in the section "Choice of Cartesian versus Semi-log Plotting" of how extrapolated values will be impacted by the way the master curve is drawn in areas where several options are suggested by individual data points. In the case of Fig. 2219-3, giving greater weight to the 700 °F data will lead to more conservative (i.e., lower) extrapolated values in this region of the curves.

A Cartesian master curve for 2219-T6 forgings was also generated using a C_{LMP} value of 25 (rounded from the calculated average of 24.7 from the isostress calculation) and is presented in Fig. 2219-4. A comparison of the extrapolated 10,000 and 100,000 h stress rupture strengths based on the two semi-log plots (Fig. 2219-3) and the Cartesian plot (Fig. 2219-4) is shown in the lower part of Table 2219-2; overall there are generally only small differences.

In summary, software systems such as Granta MI:Lab are available to aid investigators in their parametric analyses of properties such a creep and stress rupture strengths. Investigators need to be aware of the strengths and limitations of such software and apply their own judgment to the output. In addition, the illustration here using stress rupture data for 2219-T6 forgings seems to support the discussion in the section "Choice of Cartesian versus Semi-log Plotting" that semi-log plotting of master parametric curves does not seem to add appreciably to the consistency or precision of the extrapolation.

Application of LMP to Comparisons of Stress Rupture Strengths of Alloys, Tempers, and Products

While LMP analyses are usually aimed at the optimization of extrapolation for a specific alloy and temper, they can also be useful for comparing the performance of different tempers, products,

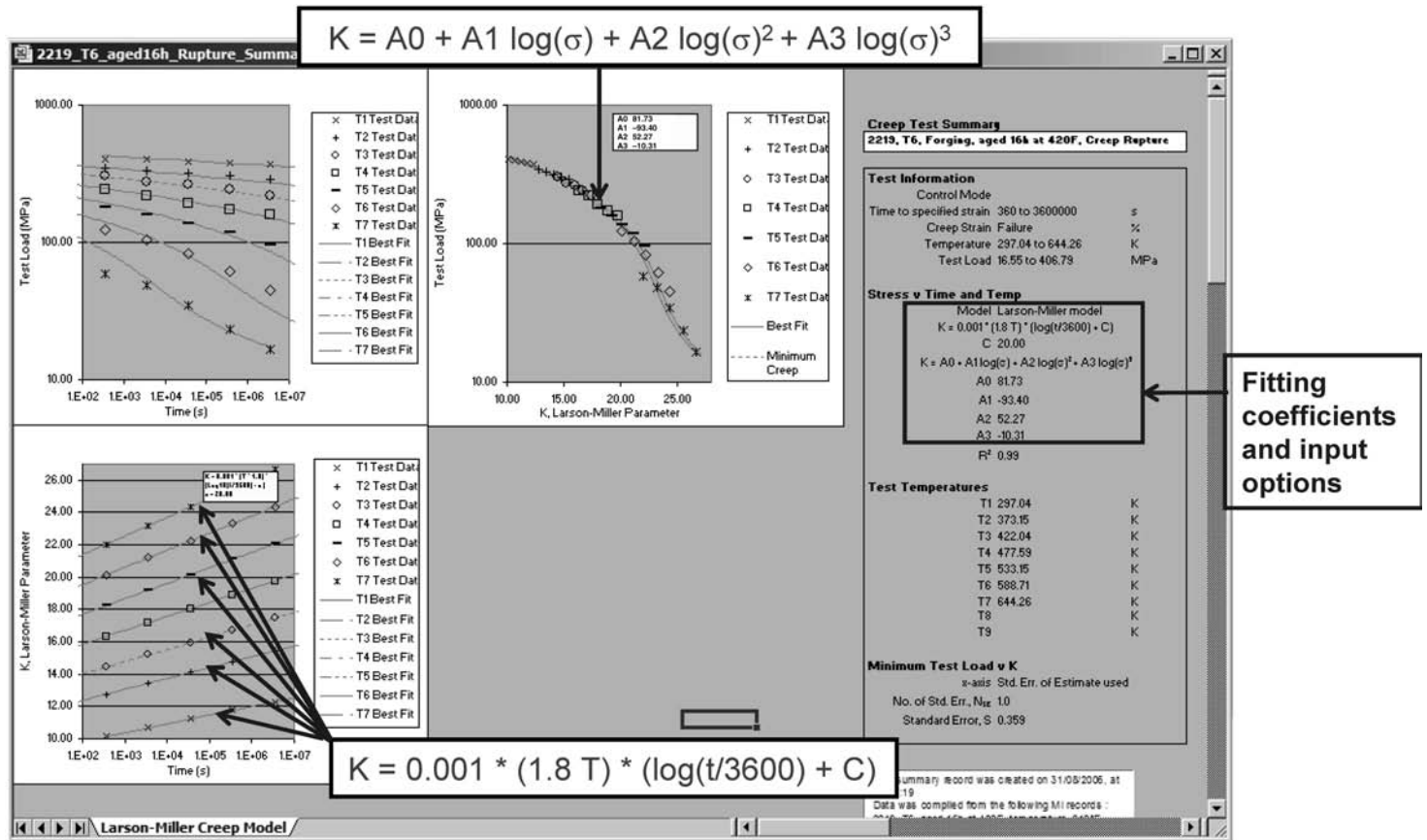


Fig. 3 Creep Summary Module presentation of stress rupture data and LMP master curve for 2219-T6 forging

or conditions of a given alloy, or for comparisons of different alloys. Several examples of such applications are described below and included in the data sets to illustrate the following types of comparisons:

- Different tempers of the same alloy
- Different products of the same alloy and temper
- Parent metal and welds of compatible filler alloys
- As-welded condition and heat treated and aged after welding
- Different alloys

The critical difference between analyzing any type of numerical data using LMP or any of the other parametric relationships is the approach to the calculation of the constant for the Larson-Miller parameter, C_{LMP} . In analyzing data for a given alloy, temper, and product, the challenge is to determine the value of C_{LMP} that provides the best fit of all of the available data for that particular material. On the other hand, in preparing for comparisons of any two or more sets of data for different lots, alloys, tempers, or conditions, the challenge is to determine a value of C_{LMP} that adequately fits both or all of the several sets involved.

As a result, in the latter case, it may sometimes be necessary to use a less-than-optimal value of C_{LMP} for one or more of the individual materials included in the comparison, but one that provides sufficiently good fit for the multiple sets involved and so provides a useful comparison.

In cases where it proves difficult or impossible to find suitable value of C_{LMP} to fit the multiple sets of data for which a comparison is being attempted, it is probably best to abandon this approach and use direct strength-life plots at individual temperatures of interest.

Comparisons of Stress Rupture Strengths of Different Tempers of an Alloy

Several opportunities exist within the archival data to compare the stress rupture strengths of two or more tempers of a single alloy.

Figure 1100-9—Comparison of 1100-O and H14. As one would expect, the LMP master curves for 1100-O and 1100-H14 converge rather smoothly at parameter values equivalent to relatively short times at 600 °F or higher and relatively long times at lower temperatures. This is associated with the gradual annealing of the 1100-H14. It is clear, however, that the H14 temper offers considerable advantage in stress rupture strength over the O temper over much of the range.

Figure 3003-12—Comparison of 3003-O, H12, H14, and H18. While the data for individual tempers of 3003 suggested slightly different “best” values of C_{LMP} , ranging from about 15 to 20 (Table 3003-2), a value of 16.6) optimum for the O temper provided a reasonable average for the group, leading to the comparisons in Fig. 3003-12. Overall, as expected, 1100-H18 showed the superior relationship. Interestingly, there was little difference in the parametric relationships for the H12 and H14 tempers, but both

were significantly superior to the O temper and about midway between the O and H18 tempers. As expected the relationships for all four tempers converged at time-temperature conditions consistent with annealing of the strain-hardened tempers.

Figure 3004-4—Comparison of 3004-O, H34, and H38. As for 3003, the relationships for various tempers of 3004 suggested somewhat different optimal values of C_{LMP} , but a value of 20 provided suitable data fit and a useful comparison for all of the tempers, as in Fig. 3004-4. The comparison of 3004-O, H34, and H38 differed somewhat from the other comparisons, however, in that the relationships for the three tempers converged at lower time-temperature combinations, and there was significant advantage of the H34 and H38 tempers over the O temper for a relatively narrower range. This suggests that perhaps the lot of 3004-O for which data were used in this study was not fully annealed to begin with and through the test program underwent additional recrystallization and softening.

Figure 5052-5—Comparison of 5052-O, H32, H34, and H38. A value of C_{LMP} of 16.0 appeared to reasonably characterize most 5052 data, and Fig. 5052-5 was generated with that constant. Significant advantages for the strain-hardened tempers existed only at relatively moderate time-temperature combinations, with convergence of the curves occurring at mid-range of the data. In this instance there was little advantage for the H38 temper over the H34 temper under any condition, but both showed some advantage over the H32 and, of course, the O temper.

Figure 5454-20—Comparison of 5454-O and H34. Figure 5454-20 shows the LMP master curve for 5454-O and H34 based on the same value of C_{LMP} as used for the O temper ($C_{LMP}=14.3$). As would be expected, the master curve and individual data points for the H34 temper blend into the original curve for the O temper as the LMP value increases, though the difference is not significant except at lower test temperatures.

Figure 6061-5—Comparison of 6061-O and T6. As with strain-hardened tempers, the master parametric curves for stress rupture strength for T6-type tempers will converge with those for the O temper as the time-temperature exposure increases. This is illustrated for 6061-T6 in Fig. 6061-5, as beyond LMP values of about 24,000, equivalent to exposures at 600 °F and above, the two curves are coincident.

Figure 6063-3—Comparison of 6063-T5 and T6. In the case of 6063, the T5 temper refers to extruded shapes that are solution heat treated and air or water quenched directly from the extrusion press, while the T6 temper is intended to designate those extruded shapes which, following extrusion, are given a separate furnace heat treatment and subsequently water quenched before aging. As illustrated in Fig. 6063-3, the T6 temper has consistently higher strengths at minimum creep rate than those of the T5 temper, as would be expected given the higher-quality heat treatment.

Comparisons of Stress Rupture Strengths of Different Products of an Alloy

Figure 6061-4—Comparison of 6061-T651 Plate and 6061-T6 Sheet and Rod. Figure 6061-4 illustrates that there can be significant differences in the stress rupture strengths of different products of some alloys. When all plotted together with a

LMP constant, C_{LMP} , of 20.3, the stress rupture strengths of 0.064 to 0.125 in thick sheet and 3/4 in. diam rolled and drawn rod were consistently higher than those of 1 to 1 1/2 in. thick 6061-T651 plate. The differences were as much as about 10 ksi at the maximum, and even at very high temperatures modest differences persisted. This magnitude of effect is unexpected since the sheet and rod would likely recrystallize more than thicker plate, usually leading to lower static strengths at room temperature.

Comparisons of Stress Rupture Strengths of Welds with Parent Alloys

Figure 5052-9—Comparison of 5052 Welds in 5052-H112 Plate with Various Tempers of 5052. The stress rupture strengths of 5052 welds in 5052-H112 plate, tested as-welded, appear from Fig. 5052-9, plotted with a C_{LMP} of 16, to be about the same as those of 5052-H32 over the lower-temperature range. In the higher-temperature, longer-exposure time range, the rupture strengths actually seem modestly higher than those of 5052 plate in various tempers, but this is probably a reflection of lot-to-lot variations more than any reliable trend. It does give confidence that the rupture strengths of welds would be at least as high as those of the parent metal over much of the higher LMP range.

Figure 5454-20—Comparison of 5454 Welds in 5454-H32 Plate with Various Tempers of 5454. Plotted in Fig. 5454-20 along with data for 5454-O and H34, the stress rupture strengths of 5454 welds in 5454-H32 plate fall very close to the relationship for 5454-O. This is as would be expected because of the softening in the weld zone resulting from the melting and resolidification of the weld metal, plus the adjacent softening in the heat-affected zone.

Figure 6061-27—Comparison of 6061-T651 Plate and 4043 Welds in 6061-T651 Plate. The stress rupture strengths of 4043 welds in 6061-T651 are largely inferior to those of the parent metal 6061-T651 plate itself, as illustrated in Fig. 6061-27. Those curves are plotted using C_{LMP} of 17.4, less than optimal for the 4043 welds, but it is nevertheless clear that as-welded 4043 joints have significantly lower strengths than the parent plate, with some difference (2–3 ksi) existing even to relatively high temperatures.

Figure 6061-28—Comparison of 4043 Welds in 6061-T651 Plate, As-Welded and Heat Treated and Aged after Welding. Heat treating and artificially aging 4043 welds in 6061-T651 plate appears from the data in Fig. 6061-28 to only modestly improve the stress rupture strength of the joints, and that effect appears significant only to relatively modest temperatures. The stress rupture strengths of the heat treated 4043 welds still fall significantly below those of the parent 6061-T651 plate.

Figure 6061-29—Comparison of 4043 and 5356 Welds in 6061-T651 Plate. No optimum value of C_{LMP} could be established permitting a completely satisfactory comparison of 4043 and 5154 welds in 6061-T651 plate; a value of $C_{LMP} = 20.3$ provided the relationships in Fig. 6061-29. In this chart, welds made with 5154 filler alloy appear significantly superior in stress rupture strength to those of 4043 welds when tested at lower temperatures, but as temperature and time at temperature increase, the advantage seems to shift to the 4043 welds. At the highest temperature for which data are available for 5154 welds, 550 °F, the advantage for 4043 welds was about 2 ksi, more than 25%.

Comparisons of Different Alloys

Figure 6061-30—Comparison of 6061-T651 and 5454-H34 plate. A reasonable comparison of interest to designers may be whether or not to use 6061-T651 plate or 5454-H34 plate for some type of tankage that requires sustained high-temperature loading. While the optimal C_{LMP} for the two alloys and tempers were not identical, a value of C_{LMP} of 16 provided reasonably good comparisons and was used in producing Fig. 6061-30. As illustrated in that figure, alloy 6061-T651 maintains a significant margin of higher performance over most of the high-temperature range.

Figure 5456-7—Comparison of Stress Rupture Strengths of Welds in 5052, 5083, and 5456. A value of C_{LMP} of 15 provided reasonable parametric relationships for 5052 welds in 5052 plate, 5183 welds in 5083 plate and 5556 welds in 5456 plate and so was used to produce Fig. 5456-7. As shown there, the stress rupture strengths of 5183 welds in 5083 and 5556 welds in 5456 are about equal over the entire range, not surprising given the close agreement in chemical compositions of these alloys. The stress rupture strengths of 5052 welds in 5052 plate were significantly lower up to LMP values of about 14,000, but at more severe time-temperature combinations leading to higher LMP values there was little difference among the stress rupture strengths of the three filler alloys. The ± 1 ksi differences would not be considered statistically significant without confirmation from much more extensive testing.

Application of LMP to High-Temperature Tensile Data for Aluminum Alloys

While the application of the Larson-Miller Parameter and time-temperature parameters to creep data, including rupture life and times to develop specific amounts of creep strain (i.e., 0.1%, 0.2%, 1%, etc.), is fairly widespread, little use is generally made of the parameters in analyzing other types of high-temperature data for aluminum alloys.

One obvious example of other high-temperature data to which the parameters might be applied is the tensile properties of aluminum alloys at temperatures above room temperature. For aluminum alloys, both the temperature and the time of exposure at temperature affect the resultant values, and the effects of time at temperature are cumulative if the exposure is alternating. As a result, graphical presentations of such data usually include a family of curves, presenting either tensile ultimate and tensile yield strengths as a function of temperature with a family of curves for different exposure time, e.g., 100, 1000, and 10,000 h, or those properties as a function of exposure time with a family of curves for each temperature. Illustrative examples of the two typical modes of graphical presentation are shown for the tensile strength and tensile yield strength of 5456-H321 in Fig. 5456-3 and 5456-4, respectively.

Since a family of curves is involved in each type of graphical presentation, a systematic means of consolidating the properties into a single continuous master curve would be of value, especially for extrapolation purposes, as with creep data.

Even before attempting such analyses, it is apparent from the plots in Fig. 5456-3 and 5456-4 that the parametric approach may

not prove useful throughout the whole range of exposure temperatures. That is primarily because, at relatively low temperatures (up to ~ 212 °F (100 °C) and at relatively higher temperatures especially (above 450 °F, or 235 °C), the properties do not vary with exposure time. It is not clear, for example, that long-time exposure at 500 °F (260 °C) will ever result in strengths as low as exposure even for short times at 600 °F (315 °C). Nevertheless, in the midrange of temperatures, there is reason to believe that the parametric approach may be fruitful.

Based on isostress calculations of the data in Fig. 5456-3 and 5456-4, which led to quite a wide range for C_{LMP} (~ 28 – 65), values of 54 and 46 were chosen for tensile strength and yield strength, respectively. The calculations of C_{LMP} led to the LMP master curves in Fig. 5456-5 and 5456-6 for tensile strength and yield strength, respectively.

The master curves for tensile strength (Fig. 5456-5) and tensile yield strength (Fig. 5456-6) look remarkably uniform and are consistent with most data points for intermediate temperatures; as expected based on the previous observations, the major exceptions were those for the relatively low and very high temperatures. It would appear that for the intermediate temperatures at least, the LMP may be a useful tool for long-exposure extrapolation, but that it must be used with caution, and with careful comparisons with other graphical means of extrapolations.

Application of LMP to Microstructural Changes and Corrosion Performance

While there has been little published on the application of parameters such as LMP to project likely microstructural changes, the usefulness of the parameters in extrapolating creep and rupture life data provide some basis for the logic that what is really being forecast are changes in microstructure. In a recent study at Secat, Inc. (Ref 16), the authors made a useful study of that potential.

The potential value of such an approach is illustrated by the experience by the U.S. Navy and Coast Guard in which ships stationed for years in equatorial environments are subjected to endless hours of on-deck temperatures approaching 150 °F (65 °C). In battle zones, high-temperature exposures are aggravated by temperature increases from gun turrets firing at regular intervals. The net result may be the equivalent of 20 to 30 years of exposure to temperatures averaging 150 °F (65 °C). Some aluminum alloys thought to be resistant to intergranular corrosion attack have experienced failures as a result of such exposures.

Aluminum-magnesium alloys containing more than 3% Mg, such as 5456-H321, were widely used in ship superstructures before about 1980 and experienced the type of failure described above. Such exposures resulted in a gradual buildup of the magnesium-bearing beta-phase precipitates along the grain boundaries of such alloys, in turn making them susceptible to grain boundary corrosion and exfoliation attack after many years of service (Ref 20). Around 1980, a new temper was developed for high-magnesium-bearing aluminum alloys, the H116 temper that was considered much more resistant to such equatorial marine exposures and easily met the requirements of applicable ASTM Standard Test

Methods such as G 66 (Ref 21) and G 67 (Ref 22), and the requirement for marine alloy plate in ASTM Standard B 928 (Ref 23). However, in recent years, more evidence of continued failures has been found.

As a result, there is a need for a more reliable means to predict the performance effects of many years of exposure on the corrosion performance of aluminum alloys. The use of LMP to project potential microstructural changes indicative of such susceptibility appears to offer a means to achieve this.

In the initial study (Ref 16), the value of C_{LMP} of 20 recommended by Larson and Miller and broadly supported in creep testing on Al-Mg alloys was selected to determine short-term exposures that might predict the microstructural conditions after 30 years of exposure at 150 °F (65 °C).

Using LMP, the exposure of about 30 years (e.g., 250,000 h) at 150 °F (610 °R; 65 °C) becomes:

$$LMP = 610(20 + \log 250,000) = 610 \times 25.383 = 15,483$$

For an equivalent rapid-response test to be complete in 4 h, the exposure temperature must be:

$$15,483/(20 + \log 4) = 15,483/20.598 = 752 \text{ °R or } 292 \text{ °F (144 °C)}$$

For an equivalent rapid-response test to be complete in 4 days (96 h), the exposure temperature must be:

$$15,483/(20 + \log 96) = 15,483/21.976 = 705 \text{ °R or } 245 \text{ °F (118 °C)}$$

These calculations utilizing the LMP suggested that relatively short-time experimental exposures of either 4 h at 292 °F (144 °C)

or 96 h at 245 °F (118 °C) may be useful in predicting the effect of marine service exposures of 30 years at temperatures up to 150 °F (65 °C).

The results of the preliminary tests to explore this approach are illustrated by the micrographs in Fig. 4. Included is the microstructure of $\frac{1}{4}$ in. thick commercially produced 5456-H116 as produced and the microstructure after exposures of 4 and 96 h exposures at 292 °F (144 °C) and 245 °F (117 °C), respectively.

The as-produced 5456-H116 shows some precipitation, but not concentrated along the grain boundaries where it would likely lead to grain-boundary corrosion attack. On the other hand, after exposure simulating 30 years at 150 °F (65 °C) per LMP analysis, there is continuous grain-boundary precipitation of the beta phase, indicating a high likelihood of some corrosion attack by either exfoliation or stress-corrosion cracking on those grain boundaries.

Thus, the LMP approach to simulating long-life service exposures on the microstructures of aluminum alloys appears to be preliminarily validated.

It appears that one step to usefully extend this study is to explore the use of a value of C_{LMP} more closely associated with tensile properties at temperatures closer to those in the microstructural study of interest, namely from 150 to 350 °F (65 to 175 °C). These considerations lead to values of C_{LMP} around 50 rather than 20, providing the following simulations of 30 years at 150 °F (65 °F):

$$\begin{aligned} \text{The critical LMP value: } LMP &= 610(50 + \log 250,000) \\ &= 610 \times 55.383 = 33,783 \end{aligned}$$

$$\begin{aligned} \text{Therefore, for a 4 h test: } 33,783/(50 + \log 4) &= 33,783/50.598 \\ &= 668 \text{ °R or } 208 \text{ °F (98 °C)} \end{aligned}$$

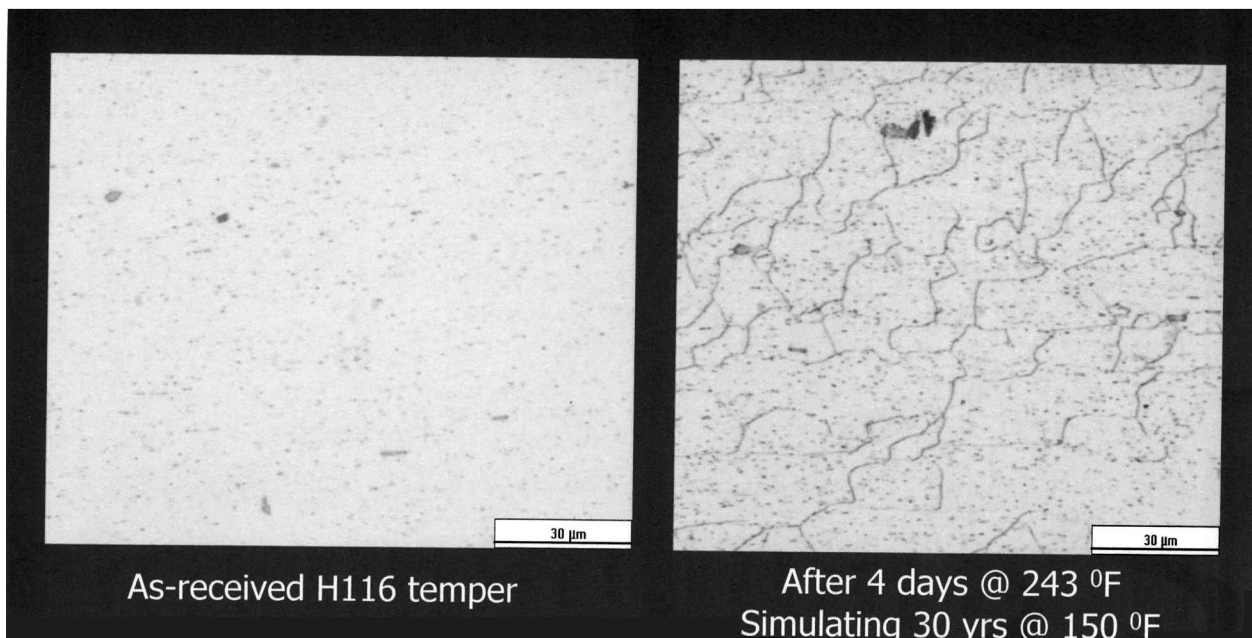


Fig. 4 Microstructure of 5456-H1161 as-fabricated and following LMP simulation of 30 years of exposure at 150 °F

$$\begin{aligned} \text{And for a 4 day test: } & 33,783/(50 + \log 96) = 33,783/51.976 \\ & = 650 \text{ }^\circ\text{R or } 190 \text{ }^\circ\text{F (87 }^\circ\text{C)} \end{aligned}$$

Examinations of microstructures of 5456-H116 plate after exposure to these short-time test periods also illustrated the grain-boundary buildup.

Obviously, it will take many years to prove conclusively whether this approach is accurate and reliable. Nevertheless, in the short term, it offers a means of estimating microstructural changes as a result of high-temperature exposures that might otherwise be completely unpredictable.

Conclusions

The usefulness of the parametric relationships such as the Larson-Miller Parameter (LMP) for the analysis and extrapolation of high-temperature data for aluminum alloys has been described herein, noting its considerable value for creep and stress rupture strength projections. Illustrations have been provided of the relatively good accuracy in using the Larson-Miller Parameter to project creep strengths from data obtained in relatively short-term tests (<10,000 h) to rupture lives as great as 1×10^6 h where actual long-term testing was carried out to verify the extrapolations.

Some limitations that must be recognized in using time-temperature parametric relationships have also been illustrated. While master parametric representations of creep and stress rupture data for aluminum alloys in tempers that do not undergo much microstructural change under the scope of conditions in the testing are very uniform and represent the data quite well, the same may not always be true for alloys in highly cold-worked or solution heat treated tempers. In the latter case, considerable care must be taken to obtain sufficiently representative data over as wide a range of test conditions as possible and considerable judgment is required in selection of the appropriate constant for the parametric relationship (C_{LMP} for the Larson-Miller Parameter).

About 100 archival Larson-Miller Parametric master curves originally developed for aluminum alloys at Alcoa Laboratories are included in this publication with Alcoa, Inc. permission. These are illustrative examples typical and representative of the respective alloys and tempers, but have no statistical basis and therefore are not to be considered as the basis for design.

An example of the application of LMP to the tensile properties of one alloy (5456-H321) has also been illustrated, indicating its limitations at relatively low temperatures (near room temperature up to ~ 212 °F, or 100 °C) or at very high temperatures (at or above 500 °F, or 260 °C), but its potential value at intermediate temperatures, say 212 to 450 °F (~ 100 to 230 °C).

An illustration has also been provided that parametric relationships such as LMP may be used to develop simulations of the possible effects of very long high-temperature service on the microstructure of aluminum alloys by defining what relatively short-term exposures might best project such changes. An example illustrating the ability to project the possible sensitization of 5456-H321 to intergranular corrosion attack after many years of service exposure at temperatures in the range of 150 °F (65 °C) has also been presented.

REFERENCES

1. H. Eyring, Viscosity, Plasticity, and Diffusion as Examples of Absolute Reaction Rates, *J. Chem Phys.*, Vol 4, 1936, p 283
2. W. Kauzmann, Flow of Solid Metals from the Standpoint of Chemical Rate Theory, *Trans. AIME*, Vol 143, 1941, p 57
3. S. Dushman, L.W. Dunbar, and H. Huthsteiner, Creep of Metals, *J. Appl. Phys.*, Vol 18, 1944, p 386
4. J.C. Fisher and C.W. McGregor, Tension Tests at Constant Strain Rate, *J. Appl. Mech.*, *Trans. ASME*, Vol 67, 1945, p A-824
5. J.C. Fisher and C.W. McGregor, A Velocity Modified Temperature for the Plastic Flow of Metals, *J. Appl. Mech.*, *Trans. ASME*, Vol 68, 1946, p A-11
6. J.H. Holloman and J.D. Lubahn, The Flow of Metals at High Temperatures, *General Electric Review*, Vol 50, Feb 1947, p 28–32; April 1947, p 44–50
7. J.H. Holloman and C. Zener, Problems in Non-Elastic Deformation of Metals, *J. Appl. Phys.*, Vol 17, Feb 1946, p 69–82
8. J.H. Holloman and L.C. Jaffe, Time-Temperature Relations in Tempering Steel, *Trans. AIME*, Iron and Steel Div., Vol 162, 1945, p 223–249
9. S.S. Manson and A.M. Haferd, “A Linear Time-Temperature Relation for Extrapolation of Creep and Stress-Rupture Data,” Technical Note 2890, NACA, March, 1953
10. F.R. Larson and J. Miller, A time-Temperature Relationship for Rupture and Creep Stresses, *Trans. ASME*, Vol 74, July 1952, p 765–771
11. S.S. Manson, “Design Considerations for Long Life at Elevated Temperatures,” Technical Report TP-1-63, NASA, 1963
12. O.D. Sherby and J.E. Dorn, Creep Correlations in Alpha Solid Solutions of Aluminum, *Trans. AIME*, Vol 194, 1952
13. K.O. Bogardus, R.C. Malcolm, and M. Holt, “Extrapolation of Creep-Rupture Data for Aluminum Alloys,” presented at 1968 ASM Materials Engineering Congress, (Detroit, MI), D8-100, American Society for Metals, 1968, p 361–390
14. *ASME Boiler and Pressure Vessel Code*, ASME, updated periodically.
15. W.C. Leslie, J.W. Jones, and H.R. Voorhees, Long Term Creep Rupture Properties of Aluminum Alloys, *ASTM Proc.*, 1980, p 32–41
16. Granta MI:Lab, product and trademark of Granta Design Ltd., Cambridge, England
17. J. Gilbert Kaufman, *Properties of Aluminum Alloys—High Temperature Creep and Fatigue Data*, ASM International, 2001
18. Alloy Center, ASM International, <http://products.asminternational.org/alloycenter/index.jsp>
19. J.G. Kaufman, Zh. Long, S. Ningileri, Application of Parametric Analyses to Aluminum Alloys, *Proc. TMS Light Metals Symposium*, TMS, Warrendale, PA, 2007
20. Corrosion of Aluminum and Aluminum Alloys, *Corrosion: Materials*, Vol 13B, *ASM Handbook*, ASM International, 2006
21. “Test Method for Visual Assessment of Exfoliation Corrosion Susceptibility of 5XXX Series Aluminum Alloys (ASSET

- Test),” G 66, *Annual Book of ASTM Standards*, Vol 03.02, ASTM International
22. “Test Method for Determining Susceptibility to Intergranular Corrosion of 5XXX Series Aluminum Alloys by Mass Loss after Exposure to Nitric Acid (NAML Test),” G 67 *Annual Book of ASTM Standards*, Vol 03.02, ASTM International
23. “Specification for High-Magnesium Aluminum Alloy Sheet and Plate for Marine Service or Similar Environments,” B 928, *Annual Book of ASTM Standards*, Vol 02.02, ASTM International

ADDITIONAL SUPPORT REFERENCES

On Aluminum and Aluminum Alloys

- *The Aluminum Association Alloy and Temper Registrations Records: Designations and Chemical Composition Limits for Aluminum Alloys in the Form of Castings and Ingot*, The Aluminum Association, Inc., Washington, DC, Jan 1996
- *The Aluminum Association Alloy and Temper Registrations Records: Tempers for Aluminum and Aluminum Alloy Products*, The Aluminum Association, Inc., Washington, DC, Feb 1995
- *Aluminum Casting Technology*, 2nd ed., The American Foundrymen’s Society, Inc., D. Zalenas, Ed., Des Plaines, IL, 1993
- *The Aluminum Design Manual*, The Aluminum Association, Arlington, VA, 2005
- *Aluminum Standards and Data*, English and Metric Editions, The Aluminum Association, Arlington, VA, 2005
- *American National Standard Alloy and Temper Designation Systems for Aluminum*, ANSI H35.1-1997, American National Standards Institute (ANSI), The Aluminum Association, Inc., Secretariat, Washington, DC, 1997
- *Applications of Aluminum Alloys*, The Aluminum Association, Arlington, VA, 2001
- *Application of Aluminum to Fast Ferries*, Alumitech 97, The Aluminum Association, Arlington, VA, 1997
- D.G. Altenpohl, *Aluminum: Technology, Applications and Environment*, The Aluminum Association Inc., and TMS, 1999
- *International Accord on Wrought Aluminum Alloy Designations*, The Aluminum Association, Inc., Washington, DC, published periodically.
- “NADCA Product Specification Standards for Die Castings Produced by the Semi-Solid and Squeeze Casting Processes,” Publication No. 403, 2nd ed., North American Die Casting Association (NADCA), Rosemont, IL 1999
- *NFFS Directory of Non-Ferrous Foundries*, Non-Ferrous Founders Society, Des Plaines, IL, 1996-7 (published periodically)
- *The NFFS Guide to Aluminum Casting Design: Sand and Permanent Mold*, Non-Ferrous Founders Society, Des Plaines, IL, 1994
- *Product Design for Die Casting in Recyclable Aluminum, Magnesium, Zinc, and ZA Alloys*, Die Casting Development Council, La Grange, IL, 1996
- *Standards for Aluminum Sand and Permanent Mold Casting*, The Aluminum Association, Inc., Washington, DC, Dec 1992

On Corrosion Resistance of Aluminum Alloys

- *Aluminum*, K.R. Van Horn, Ed., Three-volume set, American Society For Metals, 1960
- *Handbook of Corrosion Data*, 2nd ed., ASM International 1995

On Test Methods

- “Methods for Conducting Creep, Creep-Rupture, and Stress-Rupture Test of Metallic Materials,” E 139, *Annual Book of ASTM Standards*, Vol 03.01, ASTM International (updated periodically)
- “Test Methods for Tension Testing of Metallic Materials,” E 8, *Annual Book of ASTM Standards*, Vol 03.03, ASTM International (updated periodically)
- “Test Methods for Tension Testing Wrought and Cast Aluminum and Wrought and Cast Magnesium Alloy Products, B 557, *Annual Book of ASTM Standards*, Vol 02.02, ASTM International (updated periodically)